The parametric decay of Alfvén waves into shear Alfvén waves and dust lower hybrid waves

M. Jamil, H. A. Shah, M. Salimullah, K. Zubia, I. Zeba et al.

Additional information on Phys. Plasmas

The parametric decay of Alfvén waves into shear Alfvén waves and dust lower hybrid waves

M. Jamil,[1,2] H. A. Shah,[1] M. Salimullah,[1,3] K. Zubia,[1] I. Zeba,[1] and Ch. Uzma[1]

[1]*Department of Physics, Government College University, Lahore 54000, Pakistan*
[2]*Department of Physics, Crescent Model School Shadman, Lahore 54000, Pakistan*
[3]*Department of Physics, Jahangirnagar University, Savar, Dhaka 1342, Bangladesh*

The parametric decay instability of Alfvén wave into low-frequency electrostatic dust-lower-hybrid and electromagnetic shear Alfvén waves has been investigated in detail in a dusty plasma in the presence of external/ambient uniform magnetic field. Magnetohydrodynamic fluid equations of plasmas have been employed to find the linear and nonlinear response of the plasma particles for this three-wave nonlinear coupling in a dusty magnetoplasma. Here, relatively high frequency electromagnetic Alfvén wave has been taken as the pump wave. It couples with other two low-frequency internal possible modes of the dusty magnetoplasma, viz., the dust-lower-hybrid and shear Alfvén waves. The nonlinear dispersion relation of the dust-lower-hybrid wave has been solved to obtain the growth rate of the parametric decay instability. The growth rate is maximum for small value of external magnetic field $\mathbf{B_s}$. It is noticed that the growth rate is proportional to the unperturbed electron number density n_{oe}. © 2010 American Institute of Physics.
[doi:10.1063/1.3460344]

I. INTRODUCTION

The nonlinear parametric instabilities[1–3] have attained a great attention during past several decades and thoroughly investigated by the wave-wave interactions in plasmas. In recent years, dusty plasmas[4–9] have achieved a great impetus on account of the discovery of a number of fundamental modes, viz., dust acoustic wave, dust-lower-hybrid wave (DLHW),[10–14] shear Alfvén wave (SAW) (Ref. 15), etc., in dusty magnetoplasmas. Alfvén waves, the low frequency magnetohydrodynamic waves, are the most common type of waves found in the universe.[16,17] Basically, these waves are generated whenever the magnetic field lines are disturbed.

Magnetized space plasmas such as protostellar disk, molecular clouds, cometary plasmas, and stellar atmospheres support strong hydromagnetic perturbations in the form of Alfvén and magnetoacoustic waves.[18,19] Alfvén waves communicate information about the changes in magnetic field topologies and are especially important in the dynamics of magnetic reconnection. For example, changes in the auroral current magnitude and spatial configurations, or changes in the magnetospheric configuration, propagate due to Alfvén waves. Recently, rather unexpected "anomalous" ion heating has been observed during "compressional" Alfvén high harmonic fast waves heating in a controlled laboratory setting on the National Spherical Torus Experiment (NSTX). Through the three-wave interaction process, the energy of the Alfvén waves can be converted efficiently into the bulk ion species even when the Alfvén waves are not normally expected to damp.[20–24]

So far no studies have been done on the generation of electromagnetic waves off dusty plasma modes. In this paper, we have made a thorough investigation of parametric instability of the usual compressional Alfvén wave, by the electrostatic dust-lower-hybrid wave and the generation of electromagnetic shear Alfvén wave in a dusty magneto-plasma.

In Sec. II, we have solved the fluid equations of homogeneous dusty magnetoplasma in order to achieve the ponderomotive force and the coupling coefficient. In Sec. III, the nonlinear dispersion relation for the low frequency electrostatic dust-lower-hybrid wave has been derived. The dispersion relation, then, has been used to obtain the growth rate of dust-lower-hybrid wave. A numerical calculation of the growth rate of three wave parametric instability has been plotted with the typical parameters in interstellar and magnetosphere environments in Sec. IV. A brief discussion of the result has been presented in Sec. V.

II. NONLINEAR DISPERSION RELATION

We consider the propagation of a right-handed circularly polarized transverse Alfvén wave (pump wave) in a low temperature collisionless homogeneous dusty plasma in the presence of external static magnetic field, $B_s \| \hat{z}$ (Ref. 25),

$$\mathbf{E}_o = (\hat{\mathbf{x}}E_{ox} + \hat{\mathbf{y}}E_{oy})\exp[-i(\omega_o t - k_o z)], \tag{1}$$

$$E_{oy} = iE_{ox}, \tag{2}$$

$$\mathbf{B}_o = c\mathbf{k}_o \times \mathbf{E}_o / \omega_o, \tag{3}$$

$$\mathbf{k}_o = (\omega_o / \mathbf{v}_A), \tag{4}$$

$$v_A = c\omega_{ci} / \omega_{pi}, \tag{5}$$

where $\omega_o, \mathbf{k}_o$ are angular frequency and wavenumber, $\omega_{pi} = (4\pi e^2 n_{io} / m_i)^{1/2}$ is the ion plasma frequency, $\omega_{ci} = eB_s / m_i c$ is the ion cyclotron frequency, and v_A is the Alfvén speed; e, m_i, n_{io}, and c being the electronic charge, ion mass, ion number density at equilibrium, and velocity of light in a vacuum,

17, 073703-1

respectively. The propagating Alfvén wave possesses an oscillatory magnetic field, $\mathbf{B}_o = c\mathbf{k}_o \times \mathbf{E}_o / \omega_o$, which lies in the XY-plane.

We assume that the dusty plasma consists of electrons, ions, and dust particles. Electrons and ions are magnetized while the relatively massive and charged dust grains are assumed to be unmagnetized. In the presence of the pump Alfvén wave, electrons and ions acquire linear oscillatory drift velocities

$$\mathbf{v}_{oj\perp} = \frac{q_j(\mathbf{E}_{o\perp} \times \omega_{cj} - i\omega_o \mathbf{E}_{o\perp})}{m_j(\omega_{cj}^2 - \omega_o^2)}, \tag{6}$$

where j stands for electrons and ions.

On account of the hybrid motion of the magnetized electrons and ions and the unmagnetized dust particles, a low-frequency dust-lower-hybrid wave will be generated. This low-frequency electrostatic mode propagating nearly perpendicular to the static (ambient) magnetic field $\mathbf{B}_s$ is taken as perturbation $(\omega, \mathbf{k})$ and produces an electromagnetic scattered sideband shear Alfvén wave $(\omega_1, \mathbf{k}_1)$ satisfying the phase matching conditions

$$\omega_o = \omega + \omega_1,$$
$$\mathbf{k}_o = \mathbf{k} + \mathbf{k}_1. \tag{7}$$

The generated sideband in turn interacts with the pump $(\omega_o, \mathbf{k}_o)$ to produce a low-frequency ponderomotive force which amplifies and drives the low-frequency perturbation and the sideband.

The response of the plasma particles to this three-wave parametric process is governed by the fluid equations of plasmas[26]

$$\frac{\partial \mathbf{v}}{\partial t} + (\mathbf{v} \cdot \nabla)\mathbf{v} = \frac{q\mathbf{E}}{m} + \mathbf{v} \times \omega_c, \tag{8}$$

$$\frac{\partial n}{\partial t} + \nabla \cdot (n\mathbf{v}) = 0, \tag{9}$$

where $q = -e$ for electrons and $q = e$ for ions and $\omega_c = qB_s/mc$. Expressing[27]

$$\mathbf{E} = \mathbf{E}_o(\omega_o, \mathbf{k}_o) + \mathbf{E}(\omega, \mathbf{k}) + \mathbf{E}_1(\omega_1, \mathbf{k}_1),$$

$$\mathbf{B} = c\mathbf{k}_o \times \mathbf{E}_o / \omega_o + c\mathbf{k}_1 \times \mathbf{E}_1 / \omega_1,$$

$$\mathbf{v} = \mathbf{v}_o(\omega_o, \mathbf{k}_o) + \mathbf{v}(\omega, \mathbf{k}) + \mathbf{v}_1(\omega_1, \mathbf{k}_1),$$

$$n = n_o^o + n_o(\omega_o, \mathbf{k}_o) + n(\omega, \mathbf{k}) + n_1(\omega_1, \mathbf{k}_1),$$

$$\tag{10}$$

Eq. (8) yields the linear velocities. Taking common notation of q and m for electron and ion, the equation of motion for the perturbation $(\omega, \mathbf{k})$ can be written as

$$\frac{\partial \mathbf{v}}{\partial t} = \frac{q\mathbf{E}}{m} + \mathbf{v} \times \omega_c + \mathbf{F}_p, \tag{11}$$

where the ponderomotive force is given by

$$\mathbf{F}_p = \frac{i}{2}(\mathbf{k}_1 \cdot \mathbf{v}_o)\mathbf{v}_1^* - \frac{i}{2}(\mathbf{k}_o \cdot \mathbf{v}_1^*)\mathbf{v}_o + \frac{q}{2m\omega_1}\mathbf{v}_o \times (\mathbf{k}_1 \times \mathbf{E}_1^*)$$
$$+ \frac{q}{2m\omega_o}\mathbf{v}_1^* \times (\mathbf{k}_o \times \mathbf{E}_o). \tag{12}$$

Here, the asterisk "$*$" denotes complex conjugate of a quantity involved. The ponderomotive force for electrons/ions parallel to the magnetic field becomes

$$F_{pz} = \frac{q^2}{2m^2}\mathbf{E}_{o\perp} \times \omega_c \cdot \mathbf{E}_{1\perp}^*\left[\frac{k_{1\parallel}}{\omega_1(\omega_c^2 - \omega_o^2)} - \frac{k_o}{\omega_o(\omega_c^2 - \omega_1^2)}\right]$$
$$- i\frac{q^2}{2m^2}\mathbf{E}_{o\perp} \cdot \mathbf{E}_{1\perp}^*\left[\frac{k_{1\parallel}\omega_o}{\omega_1(\omega_c^2 - \omega_o^2)} - \frac{k_o\omega_1}{\omega_o(\omega_c^2 - \omega_1^2)}\right]. \tag{13}$$

Obviously, the parallel ponderomotive force on electron is larger than that on ions. Using Eqs. (8) and (9), we obtain the linear and nonlinear density perturbation as

$$n^L = -\frac{k^2\chi}{4\pi q}\phi, \tag{14}$$

$$n^{NL} = \frac{in_o q^2 k_\parallel^2}{2m^2\omega^2}\left\{\mathbf{E}_{o\perp} \times \omega_{ce}\left[\frac{k_{1\parallel}}{\omega_1(\omega_{ce}^2 - \omega_o^2)}\right.\right.$$
$$\left. - \frac{k_o}{\omega_o(\omega_{ce}^2 - \omega_1^2)}\right] - i\mathbf{E}_{o\perp}\left[\frac{k_{1\parallel}\omega_o}{\omega_1(\omega_c^2 - \omega_o^2)}\right.$$
$$\left.\left. - \frac{k_o\omega_1}{\omega_o(\omega_c^2 - \omega_1^2)}\right]\right\} \cdot \mathbf{E}_{1\perp}^*, \tag{15}$$

$$\chi = \frac{k_\perp^2}{k^2}\frac{\omega_p^2}{\omega_c^2 - \omega^2} - \frac{k_\parallel^2}{k^2}\frac{\omega_p^2}{\omega^2}. \tag{16}$$

The nonlinear current density at $(\omega_1, \mathbf{k}_1)$ can be written as

$$\mathbf{J}_1^{NL} = \frac{1}{2}n^* q\mathbf{v}_o^L,$$
$$= \frac{-\chi k^2\phi^* q^2}{8\pi m}\left(\frac{\mathbf{E}_{o\perp} \times \omega_c - i\omega_o \mathbf{E}_{o\perp}}{\omega_c^2 - \omega^2}\right). \tag{17}$$

Substituting Eqs. (14)–(17) into Poisson's equation and the wave equation, we obtain

$$\epsilon\phi = 4\pi q_e n_e^{NL}/k^2, \tag{18}$$

$$\underline{\underline{D}}_1 \cdot \mathbf{E}_1 = \frac{4\pi i\omega_1}{c^2}\mathbf{J}_1^{NL}, \tag{19}$$

where

$$\underline{\underline{D}}_1 = k_1^2\underline{\underline{I}} - \mathbf{k}_1\mathbf{k}_1 - \frac{\omega_1^2}{c^2}\underline{\underline{\epsilon}}_1, \tag{20}$$

where $\underline{\underline{I}}$ is the unit dyadic and $\underline{\underline{\epsilon}}_1$ is given by

$$\underline{\underline{\epsilon}}_1 = \begin{pmatrix} 1 - \dfrac{\omega_{pe}^2}{\omega_1^2 - \omega_{ce}^2} & \dfrac{i\omega_{pe}^2}{\omega_1^2 - \omega_{ce}^2}\dfrac{\omega_{ce}}{\omega_1} & 0 \\[3mm] -\dfrac{i\omega_{pe}^2}{\omega_1^2 - \omega_{ce}^2}\dfrac{\omega_{ce}}{\omega_1} & 1 - \dfrac{\omega_{pe}^2}{\omega_1^2 - \omega_{ce}^2} & 0 \\[3mm] 0 & 0 & 1 - \dfrac{\omega_{pe}^2}{\omega_1^2 - \omega_{ce}^2} \end{pmatrix}. \tag{21}$$

Eliminating ϕ from Eqs. (18) and (19) with straightforward calculations, we finally obtain the nonlinear dispersion relation for the low-frequency perturbation in the presence of the pump Alfvén wave as[28]

$$\epsilon = \frac{\mu}{|\underline{\underline{D}}_1|}, \tag{22}$$

where the coupling coefficient is

$$\mu = \frac{\omega_{pe}^2 |v_{oy}|^2 \omega_o^2 \omega_1 \omega_{ce} \chi k_\parallel}{2\omega^2(\omega_{ce}^2 - \omega_o^2)}$$
$$\times \left\{ \omega_{ce}\left[\frac{k_{1\parallel}}{\omega_1(\omega_{ce}^2 - \omega_o^2)} - \frac{k_o}{\omega_o(\omega_{ce}^2 - \omega_1^2)} \right] \right.$$
$$\left. - \left[\frac{k_{1\parallel}\omega_o}{\omega_1(\omega_c^2 - \omega_o^2)} - \frac{k_o\omega_1}{\omega_o(\omega_c^2 - \omega_1^2)} \right] \right\}$$
$$\times \left[\left(k_{1x}^2 - \frac{\omega_1^2}{c^2}\epsilon_{1zz} \right)\left(k_1^2 - \frac{\omega_1^2}{c^2}\epsilon_{1yy} \right) \right.$$
$$\left. + \frac{\omega_1^2}{c^2}\epsilon_{1yx}\left(k_{1x}^2 - \frac{\omega_1^2}{c^2}\epsilon_{1zz} \right) \right]. \tag{23}$$

After substituting Eq. (21) into Eq. (23), the coupling coefficient becomes as

$$\mu = -\frac{|v_{oy}/c|^2 \omega_{pe}^2 \omega_o^2 \omega_1^3 \chi k_\parallel k_1^2}{2c^2\omega^2\omega_{ce}^2}$$
$$\times \left(1 - \frac{\omega_1^2}{c^2 k_1^2} - \frac{\omega_{pe}^2 k_{1\parallel}^2}{\omega_1^2 k_1^2} + \frac{\omega_{pe}^2}{c^2 k_1^2} + \frac{\omega_{pe}^4}{\omega_1\omega_{ce}c^2 k_1^2} \right)$$
$$\times \left(\frac{k_{1\parallel}}{\omega_1} - \frac{k_o}{\omega_o} \right). \tag{24}$$

The components of the dielectric tensor at $(\omega_1, \mathbf{k}_1)$ are given by Eq. (21).

III. GROWTH RATE

In order to obtain the growth of this three-wave parametric instability, we expand $\epsilon(\omega, \mathbf{k})$ and $\underline{\underline{D}}_1(\omega_1, \mathbf{k}_1)$ around the resonant frequencies

$$\omega = \omega + i\gamma,$$

$$\omega_1 = \omega_1 + i\gamma, \tag{25}$$

$$\epsilon(\omega, \mathbf{k}) = \epsilon_r(\omega, \mathbf{k}) + i\gamma\frac{\partial\epsilon_r}{\partial\omega},$$

$$|\underline{\underline{D}}_1|(\omega_1, \mathbf{k}_1) = |\underline{\underline{D}}_1|_r(\omega_1, \mathbf{k}_1) + i\gamma\frac{\partial|\underline{\underline{D}}_1|_r}{\partial\omega_1},$$

where $\gamma \ll \omega$. At resonance $\epsilon_r = 0$ and $|\underline{\underline{D}}_1|_r = 0$ and Eq. (25) yields

$$(\gamma + \gamma_L)(\gamma + \gamma_{L1}) \equiv \frac{-\mu}{\dfrac{\partial\epsilon_r}{\partial\omega}\dfrac{\partial|\underline{\underline{D}}_1|_r}{\partial\omega_1}} \equiv \gamma_0^2, \tag{26}$$
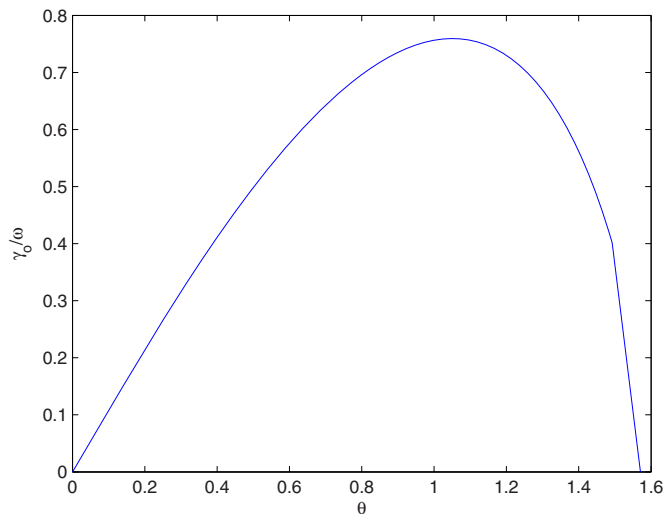
$$\frac{\partial|\underline{\underline{D}}_1|_r}{\partial\omega_1} = -\frac{2\omega_1 k_1^4}{c^2}\left(1 + \frac{\omega_{pe}^2 k_{1\parallel}^2}{c^2 k_1^4} + \frac{\omega_{pe}^2}{c^2 k_1^2} + \frac{\omega_{pe}^6}{\omega_{ce}^2 c^4 k_1^4} - 4\frac{\omega_1^2}{c^2 k_1^2} \right.$$
$$\left. - \frac{\omega_{pe}^2\omega_1^2}{c^4 k_1^4} - 6\frac{\omega_{pe}^4\omega_1^2}{\omega_{ce}^2 c^4 k_1^4} + 3\frac{\omega_1^4}{c^4 k_1^4} \right), \tag{27}$$

$$\frac{\partial\epsilon}{\partial\omega} = 2\frac{\omega_{pd}^2}{\omega^3}\left(1 + \frac{k_\parallel^2}{k^2}\frac{\omega_{pi}^2}{\omega_{pd}^2} + \frac{k_\parallel^2}{k^2}\frac{\omega_{pe}^2}{\omega_{pd}^2} \right). \tag{28}$$

Using Eqs. (27) and (28) in Eq. (26)

$$\frac{\gamma_o}{\omega} = \frac{|v_{oy}/c|^2\omega_{pe}^2\omega_1\omega_o^2\chi_e k_\parallel}{8\omega_{pd}^2\omega_{ce}^2\omega k_1} \times \frac{\left(\dfrac{k_{1\parallel}}{k_1} - \dfrac{k_o\omega_1}{k_1\omega_o} \right)\left(1 - \dfrac{\omega_1^2}{c^2 k_1^2} - \dfrac{\omega_{pe}^2 k_{1\parallel}^2}{\omega_1^2 k_1^2} + \dfrac{\omega_{pe}^2}{c^2 k_1^2} + \dfrac{\omega_{pe}^4}{\omega_1\omega_{ce}c^2 k_1^2} \right)}{\left(1 + \dfrac{k_\parallel^2}{k^2}\dfrac{\omega_{pi}^2}{\omega_{pd}^2} + \dfrac{k_\parallel^2}{k^2}\dfrac{\omega_{pe}^2}{\omega_{pd}^2} \right)\left(1 + \dfrac{\omega_{pe}^2 k_{1\parallel}^2}{c^2 k_1^4} + \dfrac{\omega_{pe}^2}{c^2 k_1^2} + \dfrac{\omega_{pe}^6}{\omega_{ce}^2 c^4 k_1^4} - 4\dfrac{\omega_1^2}{c^2 k_1^2} - \dfrac{\omega_{pe}^2\omega_1^2}{c^4 k_1^4} - 6\dfrac{\omega_{pe}^4\omega_1^2}{\omega_{ce}^2 c^4 k_1^4} + 3\dfrac{\omega_1^4}{c^4 k_1^4} \right)}. \tag{29}$$

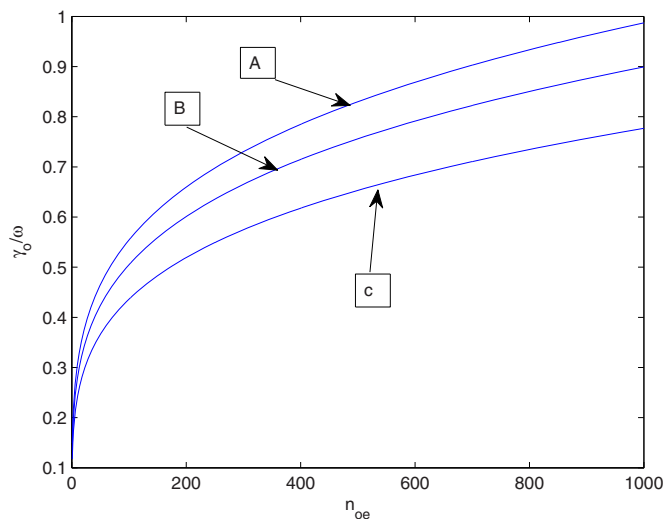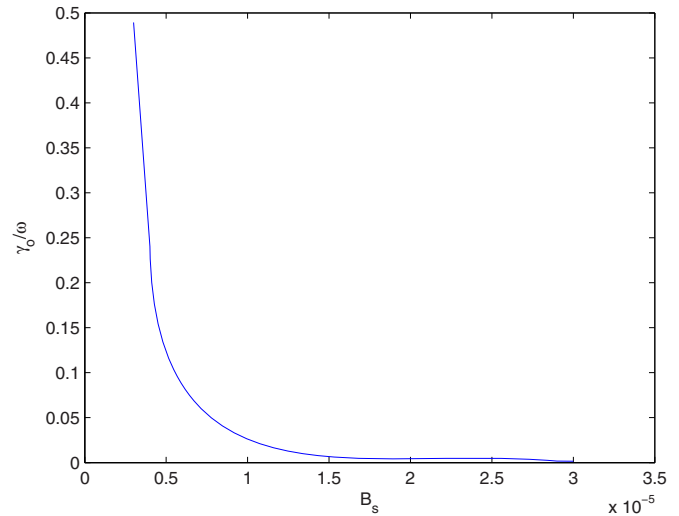Now we make numerical calculations of γ_o/ω as a function of various parameters of interest in the dusty magnetoplasma.

FIG. 1. (Color online) Relationship of normalized growth rate γ_o/ω vs θ.

FIG. 3. (Color online) Relationship of normalized growth rate γ_o/ω vs $\mathbf{B_s}$.

IV. NUMERICAL RESULTS AND GRAPHICAL DESCRIPTION

To gain some numerical appreciation of the results of our theory, we have made calculations of the growth rates for dust-lower-hybrid $(\omega, \mathbf{k})$ wave for the following set of typical parameters in cgs system: $B_s = (3-30) \times 10^{-6}$ G, $m_{oi}/m_{oe} = 1836$, $m_{od}/m_{oi} = (10^4 - 10^6)$, $n_{oe} = (10^0 - 10^3)$ cm^{-3}, $n_{od} = 10^{-7}$ cm^{-3}, $v_{oy}/c = 10^{-5}$, $w_o = 10^2$ s^{-1}, $z_d = (10^3 - 10^5)$, and scattering angle, $\theta = 0 - \pi/2$ rad.

The results of our calculations are depicted in the form of curves in Figs. 1–3. Figure 1 shows the variation γ_o/ω as a function of the angle of scattering θ. It follows that the normalized growth rate of the three-wave parametric instability first increases up to scattering angle $\pi/3$ and then decreases. It may be described that the phase matching conditions [cf. Eq. (7)] are exactly valid for particular scattering angle. Otherwise, the pump wave scatters into other possible modes which are not of our interest in this paper.

Figure 2 illustrates the variation of γ_o/ω as a function of the number density n_{oe}. It is evident from the figure that the

FIG. 2. (Color online) Relationship of normalized growth rate γ_o/ω vs n_{oe}.

normalized growth rate increases with increasing the number density. Curves A, B, and C are for $\theta = \pi/3$, $\pi/4$, and $\pi/5$, respectively. Higher number density contributes for larger energy which in turn results the growth of wave.

Figure 3 shows the nature of variation of γ_o/ω as a function of magnetic field $\mathbf{B_s}$. In this case, the behavior of the curve is found to be sensitive for higher values of $\mathbf{B_s}$. It is clear from Eq. (6) that an increase of $\mathbf{B_s}$ causes to reduce the oscillatory drift velocities for jth species, which results in decreasing the growth rate of perturbation $(\omega, \mathbf{k})$.

V. DISCUSSION

In this paper, we have investigated the parametric decay instability of the Alfvén wave into a low-frequency electrostatic dust-lower-hybrid wave propagating nearly transverse to the direction of static magnetic field and another electromagnetic sideband, viz., the shear Alfvén wave propagating nearly along the direction of the magnetic field in a cold dusty magnetoplasma. The hydrodynamic model with static magnetic field has been employed to obtain linear and nonlinear response of electrons and ions. The dust is assumed to be charged and unmagnetized.

A ponderomotive force is developed due to beating of the incident pump wave with generated sideband, to drive the low-frequency dust-lower-hybrid wave. The overall growth rate increases up to the certain value of scattering angle $(\theta = \pi/3)$, between $\mathbf{k_1}$ and the magnetic field $\mathbf{B_s}$, and above this limit it decreases. At the scattering angles for which growth rate decreases, the pump wave scatters and becomes broadened that may result in another Alfvén wave of comparatively low-frequency. It is also observed that the growth rate is a sensitive function of $\mathbf{B_s}$. Higher growth rate of electrostatic dust-lower-hybrid wave is achieved for small values of $\mathbf{B_s}$. On increasing $\mathbf{B_s}$ the instability provides some channel for damping of the dust-lower-hybrid wave. It is also noticed that the nonlinear growth rate of the parametric instability is proportional to the amplitude of the pump wave, which affects the stability properties of linear system drastically, and unperturbed electron number density n_{oe}.

The important contribution of this study is to provide further physical insight the parametric instabilities in dusty magnetoplasmas. A numerical calculation of the growth rate of the three wave parametric instability has been made with typical parameters in interstellar and magnetosphere environment.

ACKNOWLEDGMENTS

[1]M. P. Hertzberg, N. F. Cramer, and S. V. Vladimirov, Phys. Plasmas **10**, 3160 (2003).
[2]S. V. Vladimirov and S. I. Popel, Phys. Scr. **50**, 161 (1994).
[3]M. Porkolab, J. J. Schuss, B. Lloyd, Y. Takase, S. Texter, P. Bonoli, C. Fiore, R. Gandy, D. Gwinn, B. Lipschultz, E. Marmar D. Pappas, R. Parker, and P. Pribyl, Phys. Rev. Lett. **53**, 450 (1984).
[4]C. K. Goertz, Rev. Geophys. **27**, 271, doi:10.1029/RG027i002p00271 (1989).
[5]T. G. Northrop, Phys. Scr. **45**, 475 (1992); U. de Angelis, *ibid.* **45**, 465 (1992).
[6]D. A. Mendis and M. Rosenberg, Annu. Rev. Astron. Astrophys. **32**, 419 (1994).
[7]P. K. Shukla, Phys. Plasmas **8**, 1791 (2001).
[8]D. A. Mendis, Plasma Sources Sci. Technol. **11**, A219 (2002).
[9]R. L. Merlino and J. A. Goree, Phys. Today **57**(7), 32 (2004).
[10]N. N. Rao, P. K. Shukla, and M. Y. Yu, Planet. Space Sci. **38**, 543 (1990).
[11]P. K. Shukla and V. P. Silin, Phys. Scr. **45**, 508 (1992); M. Nambu, S. V. Vladimirov, and P. K. Shukla, Phys. Lett. A **203**, 40 (1995).
[12]M. Salimullah and A. Sen, Phys. Lett. A **163**, 82 (1992).
[13]M. Salimullah, M. H. A. Hassan, and A. Sen, Phys. Rev. A **45**, 5929 (1992).
[14]P. K. Shukla, Phys. Scr. **45**, 504 (1992).
[15]K. Zubia, M. Jamil, and M. Salimullah, Phys. Plasmas **16**, 094501 (2009).
[16]K. Zubia, N. Rubab, H. A. Shah, M. Salimullah, and G. Murtaza, Phys. Plasmas **14**, 032105 (2007).
[17]N. F. Cramer, *The Physics of Alfvén Waves* (Wiley-VCH, Berlin, 2001), p. 58.
[18]L. Spitzer, Jr., *Physical Processes in the Interstellar Medium* (Wiley-VCH, Weinheim, 2004), p. 256.
[19]W. Pilipp, T. W. Hartquist, O. Havnes, and G. E. Morfill, Astrophys. J. **314**, 341 (1987).
[20]T. M. Biewer, R. E. Bell, R. Feder, D. J. Johnson, and R. W. Palladino, Rev. Sci. Instrum. **75**, 650 (2004).
[21]J. V. Hollweg, Rev. Geophys. Space Phys. **16**, 689, doi:10.1029/RG016i004p00689 (1978).
[22]E. Marsch, Living Rev. Sol. Phys. **3**, 1 (2006).
[23]S. R. Cranmer and A. A. Ballegooijen, Astrophys. J. **594**, 573 (2003).
[24]S. P. Gary, L. Yin, and D. Winske, J. Geophys. Res. **111**, A06105, doi:10.1029/2005JA011552 (2006).
[25]A. K. Banerjee, S. M. Khurshed Alam, M. N. Alam, and M. Salimullah, Phys. Rev. B **37**, 1180 (1988).
[26]Md. Salimullah, R. R. Sharma, and V. K. Tripathi, Appl. Phys. (Berlin) **25**, 361 (1981).
[27]M. S. Sodha, A. K. Ghatak, and V. K. Tripathi, Prog. Opt. **XIII**, 169 (1976).
[28]Md. Salimullah and T. Singh, J. Phys. Chem. Solids **43**, 1087 (1982).